Reinforcement Learning-Based Optimal Nonlinear Control for Magnetic Levitation

Syed Tariq Naqshbandi, Huzaifah Abbas* and Dania Zaman

***Abstract*— Magnetic levitation (Maglev) systems are a testbed for advanced control strategies because of their nonlinearity, open-loop instability, and high dynamics. Accurate position control of the levitated object is a difficult task, especially under parameter uncertainties and disturbances. Traditional control approaches, like proportional-integral-derivative (PID) control, are based on linearization of the system and hence suffer from poor performance in the presence of nonlinearities. Sliding mode control (SMC) is a robust nonlinear control method that provides good disturbance rejection and parameter uncertainty tolerance. However, its performance is sensitive to the choice of controller gains, which is often a time-consuming and suboptimal manual task. To overcome this challenge, previous research has used metaheuristic algorithms, like genetic algorithms (GA), for gain tuning. These approaches enhance tracking accuracy and transient response, but are offline and non-adaptive to dynamic system changes. In this work, a Deep Deterministic Policy Gradient (DDPG) reinforcement learning approach is developed for online gain tuning of SMC in a nonlinear Maglev system. The DDPG agent engages in continuous interaction with the environment to learn an optimal policy for gain adaptation in response to system dynamics. Asymptotic stability of the closed-loop system is analyzed using Lyapunov's stability theorem for fixed gains, and the adaptive gain case is discussed. The proposed DDPG-tuned SMC is shown to have better tracking performance, shorter settling time, and better disturbance rejection and parameter uncertainty tolerance than the GA-tuned SMC through simulation studies.**

I. INTRODUCTION

Magnetic levitation systems (MLS) have attracted considerable research interest over the past few decades owing to their wide-ranging applications in engineering and technology. These include high-speed maglev trains [1], magnetic bearings [2], precision motion systems, biomedical devices, and contactless suspension mechanisms [3]. The fundamental operating principle of MLS relies on the generation of a controlled electromagnetic force to counteract gravity and maintain a ferromagnetic object at a desired position in mid-air. Despite this simplicity, MLS exhibits strong nonlinearity, open-loop instability, and fast dynamics, making precise control a challenging research problem [1], [4].

A wide range of control strategies has been developed for MLS. Classical linear controllers such as PID and state feedback methods remain widely used due to their simplicity and ease of implementation [5]. However, these methods rely on linearization around a fixed operating point and therefore suffer performance degradation under parameter variations and disturbances [6]. To address these limitations, advanced nonlinear and optimal control techniques such as model predictive control and robust control strategies have been proposed [7]. In addition, optimization-based nonlinear tracking strategies have been explored for improved performance under uncertainty [2].

Among nonlinear control techniques, sliding mode control (SMC) has emerged as one of the most effective approaches for MLS due to its strong robustness against uncertainties and disturbances [8]. SMC forces system trajectories onto a predefined sliding surface and guarantees stability using Lyapunov theory [9]. Various improved SMC structures have been developed, including adaptive and super-twisting formulations to enhance robustness and dynamic performance [10], [11]. Recent studies have also explored fuzzy inversion-based adaptive control to improve tracking accuracy in MLS [12].

A key limitation of SMC is chattering and parameter tuning difficulty. To mitigate this, metaheuristic optimization techniques have been widely adopted for controller tuning. Genetic algorithms and other evolutionary optimization techniques have been extensively used for nonlinear control systems, improving transient response and robustness [13]. Other bio-inspired and fractional-order optimization approaches, including the zebra optimization algorithm and ant colony optimization, have also been explored for SMC and PID tuning in MLS, demonstrating measurable improvements in transient response [14], [15].

Despite these advances, most optimization methods remain offline and cannot adapt to time-varying system dynamics. Reinforcement learning (RL) has recently emerged as a powerful data-driven paradigm for nonlinear system control, enabling agents to learn optimal policies through interaction with the environment [16]. Deep reinforcement learning methods such as Deep Deterministic Policy Gradient (DDPG) are particularly suitable for continuous control problems due to their actor–critic structure and function approximation capability [17]. Recent advances in adaptive SMC have further extended its capabilities; for instance, fractional-order adaptive sliding mode approaches have demonstrated effective tracking and synchronization with predefined-time stability guarantees [18]. While RL has been applied to direct control of dynamical systems, its use for online adaptive gain tuning of SMC in MLS combining the robustness guarantees of SMC with the adaptability of RL remains relatively underexplored in the literature.

Motivated by these limitations, this paper proposes a DDPG-based reinforcement learning framework for real-time adaptive tuning of sliding mode control gains in a nonlinear

*Corresponding author. Authors are with the National University of Sciences and Technology, Islamabad huzaifah.abbas@hotmail.com

magnetic levitation system. The proposed method combines the robustness of SMC with the adaptability of RL to handle uncertainties and disturbances effectively. Lyapunov-based stability analysis is presented for the fixed-gain case, and the time-varying gain scenario introduced by DDPG is discussed as a practical consideration. Performance is validated in MATLAB/Simulink under disturbance and noise conditions.

The rest of the paper is organized as follows. Section II presents the nonlinear mathematical model of the MLS. Section III describes the SMC design and optimization algorithms. Section IV presents simulation results, and Section V concludes the paper.

II. MATHEMATICAL MODELING OF MAGNETIC LEVITATION SYSTEM

The magnetic levitation system (MLS) consists of a ferromagnetic ball, an electromagnetic coil generating levitation force, a position sensor, and a power driver circuit controlled by a microcontroller. The schematic is shown in Fig. 1. Key variables include: coil inductance L (H), resistance R (Ω), source voltage E (V), coil current I (A), electromagnetic force F_E (N), gravitational force F_G (N), ball position x (m), and ball mass m (kg).

A. Mechanical Dynamics

Applying Newton's second law to the levitated ball gives:

$$m\ddot{x} = F_G - F_E \tag{1}$$

where $F_G = mg$, $g = 9.81$ m/s^2 is gravitational acceleration, and F_E is the upward electromagnetic force given by:

$$F_E = \frac{1}{2} I^2 \frac{dL(x)}{dx} \tag{2}$$

The inductance varies nonlinearly with position and is approximated as $L(x) = 2k/x^2$, where k (Nm^2/A^2) is the electromagnetic force constant. This yields:

$$F_E = k\left(\frac{I}{x}\right)^2 \tag{3}$$

and the mechanical equation of motion becomes:

$$\ddot{x} = g - \frac{k}{m}\left(\frac{I}{x}\right)^2 \tag{4}$$

B. Electrical Dynamics

Applying Kirchhoff's voltage law to the coil circuit:

$$E = IR + \frac{d}{dt}[L(x)I] \tag{5}$$

Substituting $L(x)$ and expanding the time derivative yields the current dynamics:

$$\dot{I} = -\frac{R}{L}I - \frac{2k}{L}\frac{I\dot{x}}{x^2} + \frac{E}{L} \tag{6}$$

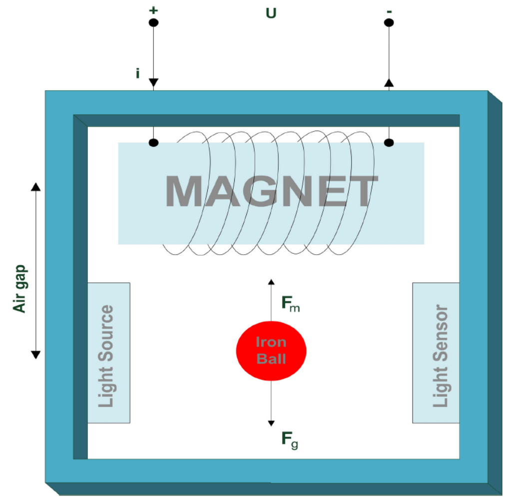

Fig. 1: Circuit diagram of the Maglev system [8].

C. State-Space Representation

Defining states $x_1 = x$ (position), $x_2 = \dot{x}$ (velocity), $x_3 = I$ (current), and control input $U = E$ (voltage), the MLS state equations are:

$$\dot{x}_1 = x_2, \quad \dot{x}_2 = g - \frac{kx_3^2}{mx_1^2}, \quad \dot{x}_3 = -\frac{R}{L}x_3 + \frac{2kx_2x_3}{Lx_1^2} + \frac{U}{L} \tag{7}$$

with output $y = x_1$. System parameters are listed in Table I.

D. Coordinate Transformation to Canonical Form

To expose a strict-feedback structure, define new coordinates:

$$z_1 = x_1, \quad z_2 = x_2, \quad z_3 = g - \frac{kx_3^2}{mx_1^2} \tag{8}$$

The transformed dynamics are $\dot{z}_1 = z_2$, $\dot{z}_2 = z_3$, and:

$$\dot{z}_3 = f(z) + g(z)U \tag{9}$$

where $f(z)$ captures the lumped nonlinearities and $g(z)$ is the input gain:

$$f(z) = \frac{2kRx_3^2}{mx_1^2L} - \frac{4k^2x_2x_3^2}{mx_1^4L} + \frac{2kx_2x_3^2}{mx_1^3}, \quad g(z) = -\frac{2kx_3}{mx_1^2L} \tag{10}$$

The control input U appears only in the third-order dynamics, giving the system a relative degree of three and making it directly amenable to sliding mode controller design.

TABLE I: Parameters of the MLS [8]

Parameter	Symbol	Value
Ball Mass	m	0.36 kg
Coil Inductance	L	0.12 H
Coil Resistance	R	9 Ω
Force Constant	k	0.00013 Nm^2/A^2
Gravity Acceleration	g	9.81 m/s^2

III. CONTROLLER DESIGN

A. Sliding Mode Control

Let $e = x_1 - x_d$ denote the position tracking error, where x_d is the desired reference trajectory, and let $\dot{e}$, $\ddot{e}$ denote its first and second time derivatives. The sliding surface is defined as:

$$s = c_1 e + c_2 \dot{e} + c_3 \ddot{e} \tag{11}$$

where $c_1, c_2, c_3 > 0$ are chosen such that the polynomial $c_1 + c_2\lambda + c_3\lambda^2$ is Hurwitz, ensuring that $s = 0$ defines a stable manifold.

The control law is composed of an equivalent term U_{eq}, derived by setting $\dot{s} = 0$ and solving for U, and a discontinuous switching term:

$$U = U_{eq} - \frac{\eta}{g(z)}\,\mathrm{sat}\left(\frac{s}{\phi}\right) \tag{12}$$

where $\eta > 0$ is the switching gain and $\phi > 0$ is the boundary layer thickness introduced to replace the sign function and mitigate chattering.

Stability Analysis (Fixed Gains): Consider the Lyapunov candidate $V = \frac{1}{2}s^2 \geq 0$. Its time derivative along the closed-loop trajectories satisfies:

$$\dot{V} = s\dot{s} = s\big(c_1\dot{e} + c_2\ddot{e} + c_3(f(z) + g(z)U - \dddot{x}_d)\big) \tag{13}$$

Substituting the control law and using $|f(z) - f_{nom}| \leq \delta$ for some bounded uncertainty δ:

$$\dot{V} \leq -\eta|s| + \delta|s| \leq -(\eta - \delta)|s| \tag{14}$$

Choosing $\eta > \delta$ ensures $\dot{V} \leq -(\eta - \delta)|s| < 0$ for $s \neq 0$, which guarantees asymptotic convergence of the tracking error to the sliding surface. It is noted that this proof assumes fixed gains $c_1, c_2, c_3, \eta, \phi$. When gains are adapted online by the DDPG agent, the system becomes time-varying; formal stability guarantees in this case require additional analysis and are considered a direction for future work.

1) Genetic Algorithm-Based Gain Tuning: To provide a baseline, a Genetic Algorithm (GA) is employed for offline tuning of the SMC parameters [13]. GA minimizes a performance index based on tracking error and control effort. The GA convergence curve and best-found parameter set are shown in Fig. 2, and the resulting optimized gains are listed in Table II. Although GA improves performance over manual tuning, its offline nature prevents adaptation to time-varying dynamics during operation.

TABLE II: Genetic Algorithm Optimized SMC Parameters

Parameter	Symbol	Value
Sliding coefficient 1	c_1	48
Sliding coefficient 2	c_2	3.7
Sliding coefficient 3	c_3	9.8
Switching gain	η	2.1
Boundary layer	ϕ	3.3

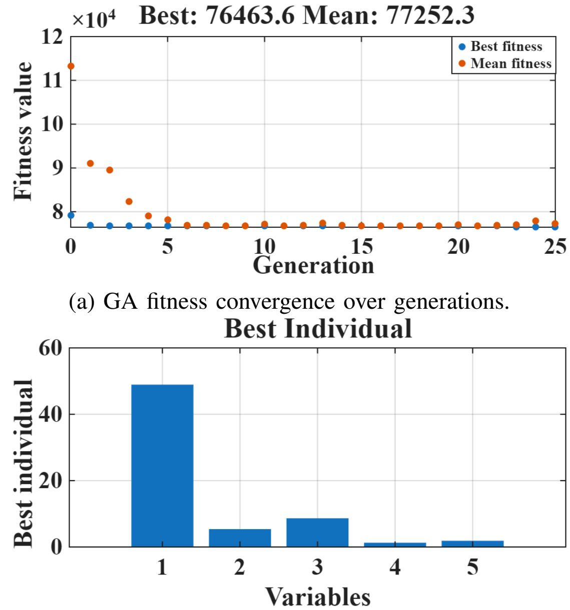

(a) GA fitness convergence over generations.

(b) Best individual: optimized gain values.

Fig. 2: Genetic algorithm optimization results.

B. DDPG-Based Gain Optimization

A Deep Deterministic Policy Gradient (DDPG) reinforcement learning framework is proposed for real-time adaptive tuning of the SMC gains. DDPG is a model-free, off-policy actor–critic algorithm for continuous action spaces [17]. At each time step, the actor network outputs updated SMC gains based on the current system state, while the critic network evaluates the long-term quality of the selected gains.

1) State and Action Space: The observation vector provided to the agent is:

$$\mathcal{S}_t = [e(t),\ \dot{e}(t),\ \ddot{e}(t),\ s(t)]^T \tag{15}$$

where $e = x_1 - x_d$ is the position error, $\dot{e}$ and $\ddot{e}$ are its derivatives, and s is the sliding variable. The action vector is the set of SMC gains to be tuned:

$$\mathcal{A}_t = [c_1,\ c_2,\ c_3,\ \eta,\ \phi]^T \tag{16}$$

Actions are constrained within the bounds given in Table III, which implicitly restricts the gain space to values known to preserve closed-loop stability.

TABLE III: DDPG Action Space Bounds

Parameter	Symbol	Min	Max
Sliding coefficient 1	c_1	0.1	50
Sliding coefficient 2	c_2	0.1	50
Sliding coefficient 3	c_3	0.1	50
Switching gain	η	0.1	20
Boundary layer	ϕ	0.01	1

2) Reward Function: The reward function penalizes tracking error and control effort:

$$r_t = -\big(\alpha_1 e^2(t) + \alpha_2 s^2(t) + \alpha_3 \dot{e}^2(t) + \alpha_4 U^2(t)\big) \tag{17}$$

Weighting coefficients $\alpha_i > 0$ are listed in Table IV.

TABLE IV: Reward Function Weighting Coefficients

Term	Symbol	Value
Tracking error	α_1	10
Sliding surface	α_2	5
Error derivative	α_3	1
Control effort	α_4	0.1

3) Network Architecture: The actor and critic networks are implemented as feedforward neural networks. The actor maps the 4-dimensional observation to the 5-dimensional action. The critic evaluates a state–action pair and outputs a scalar Q-value. The architectures are summarized in Table V.

TABLE V: DDPG Neural Network Architecture

Network	Layer	Units	Activation
Actor	Input	4	—
	Hidden (FC)	64	ReLU
	Hidden (FC)	32	ReLU
	Output (FC)	5	Tanh
Critic	Obs. Input	4	—
	Obs. FC	64	ReLU
	Obs. FC	32	—
	Act. Input	5	—
	Act. FC	32	—
	Add + ReLU	32	ReLU
	Output (FC)	1	Linear

4) Learning Mechanism: The actor and critic maintain target networks for stable training. Target network parameters θ' are updated via soft updates:

$$\theta' \leftarrow \tau\theta + (1-\tau)\theta' \tag{18}$$

The critic minimizes the temporal difference (TD) error using minibatch samples drawn from an experience replay buffer, while the actor gradient ascends the expected Q-value. Training hyperparameters are listed in Table VI.

TABLE VI: DDPG Training Hyperparameters

Hyperparameter	Value
Actor learning rate	1×10^{-4}
Critic learning rate	1×10^{-3}
Discount factor γ	0.99
Soft update coefficient τ	0.005
Replay buffer size	10^6
Mini-batch size	64
Episode length	200 steps
Maximum training episodes	500
OU noise θ_{OU}	0.15
OU noise σ_{OU}	0.2

At each control step, the trained actor generates updated gains $[c_1, c_2, c_3, \eta, \phi]$, which are applied to the SMC in real time, enabling continuous adaptation to system dynamics and disturbances without manual retuning.

IV. RESULTS

This section evaluates the proposed DDPG-SMC framework through MATLAB/Simulink simulations and compares it against conventional SMC and GA-optimized SMC. All three controllers are tested on the same nonlinear MLS model under identical initial conditions and reference trajectories. Note that conventional SMC is excluded from the disturbance rejection and parameter uncertainty tests (Sections IV-E and IV-F) because its fixed, manually tuned gains did not yield stable closed-loop behaviour under the applied perturbations; comparisons in those sections are therefore between DDPG-SMC and GA-SMC only.

A. Tracking Performance

The air-gap response in Fig. 3 shows that all three controllers achieve convergence to the desired reference. However, significant differences appear in transient behavior. Conventional SMC exhibits sensitivity to gain selection, resulting in larger overshoot. The GA-SMC improves settling time and reduces overshoot through offline-optimized gains. The proposed DDPG-SMC achieves the fastest convergence and smallest steady-state error among the three, due to its ability to continuously adapt gains in response to the evolving system state.

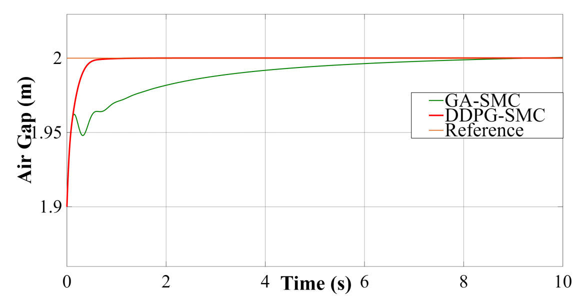

Fig. 3: Air gap x_1 (ball position) tracking response: DDPG-SMC vs. GA-SMC vs. SMC.

B. Control Effort and Smoothness

The control input signals are compared in Fig. 4. Conventional SMC produces noticeable chattering due to discontinuous switching. GA-SMC reduces chattering to some extent through optimized gain selection. The proposed DDPG-SMC produces the smoothest control action, with significantly reduced high-frequency switching, owing to the adaptive boundary layer and gain tuning performed online.

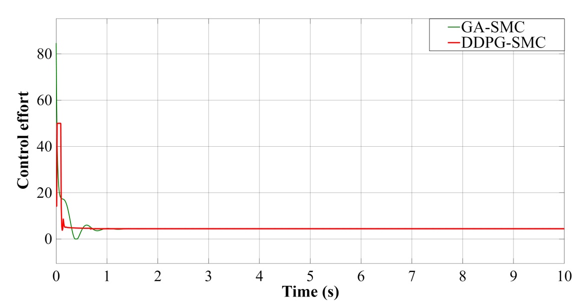

Fig. 4: Control input U (V): DDPG-SMC vs. GA-SMC vs. SMC.

C. State Response Analysis

The ball velocity response shown in Fig. 5 and the coil current response in Fig. 6 further validate the performance differences. DDPG-SMC exhibits smoother transient evolution with reduced oscillations in both states compared to GA-SMC and conventional SMC, indicating improved damping and energy efficiency under RL-based adaptation.

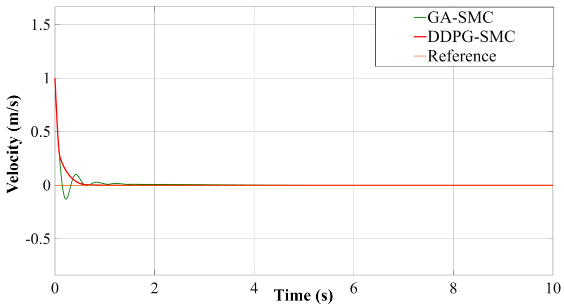

Fig. 5: Ball velocity x_2 response: DDPG-SMC vs. GA-SMC vs. SMC.

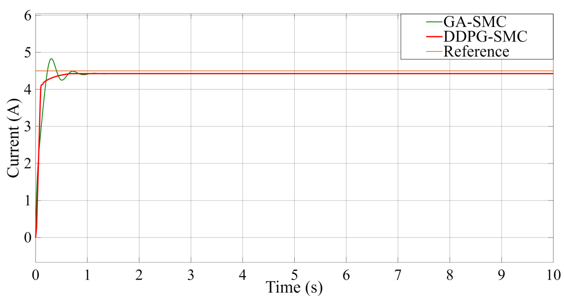

Fig. 6: Coil current x_3 response: DDPG-SMC vs. GA-SMC vs. SMC.

D. Summary

The simulation results confirm that: (i) conventional SMC provides robustness but is sensitive to gain tuning; (ii) GA-SMC improves performance but is limited by its offline, static nature; and (iii) DDPG-SMC achieves the best tracking accuracy, smoothest control input, and most consistent state response, validating the effectiveness of online RL-based gain adaptation for nonlinear control.

E. Disturbance Rejection Analysis

To evaluate robustness under external disturbances, a combined sinusoidal and white noise disturbance signal with a smooth trapezoidal envelope was injected into the ball acceleration dynamics ($\dot{x}_2$) over two windows: a positive disturbance from $t = 5$–8 s and a negative disturbance from $t = 9$–11 s, with a peak amplitude of ± 1.3 N/kg. Fig. 7 shows the air gap response and Fig. 8 shows the velocity response under disturbance.

DDPG-SMC maintains a smaller peak deviation in position and recovers to the reference faster than GA-SMC after both disturbance windows. The velocity response in Fig. 8

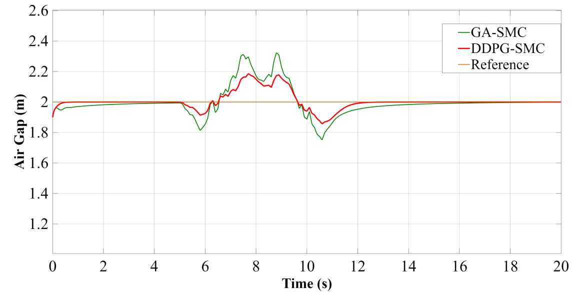

Fig. 7: Air gap x_1 response under external disturbance: DDPG-SMC vs. GA-SMC.

further highlights the advantage — GA-SMC exhibits oscillations reaching ± 0.7 kg·m/s, while DDPG-SMC constrains velocity deviations to within ± 0.2 kg·m/s, demonstrating superior disturbance attenuation through online gain adaptation.

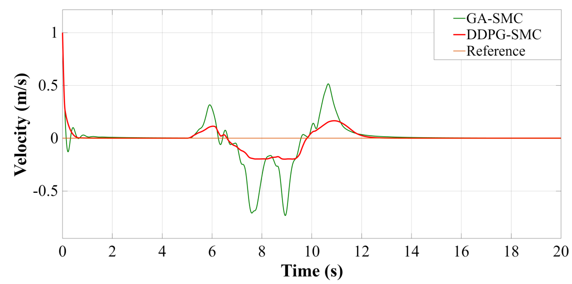

Fig. 8: Ball velocity x_2 response under external disturbance: DDPG-SMC vs. GA-SMC.

F. Parameter Uncertainty Analysis

To assess robustness to model uncertainty, the ball mass m and coil resistance R were each varied by $\pm 20\%$ from their nominal values while keeping all controller gains fixed. Figs. 9 and 10 show the air gap tracking response under mass and resistance variations, respectively.

Under mass variation (Fig. 9), GA-SMC exhibits significant steady-state offset under both $+20\%$ and -20% perturbations, with the -20% case diverging notably from the reference. DDPG-SMC maintains tracking much closer to the reference under the same variations, with only a small transient offset under $+20\%$ mass increase. Similar behavior is observed under resistance variation (Fig. 10), where GA-SMC shows persistent steady-state error while DDPG-SMC converges near the reference in both perturbed cases. These results confirm that the adaptive gain mechanism of DDPG-SMC provides inherently better robustness to parameter uncertainty compared to the fixed offline gains of GA-SMC.

V. CONCLUSIONS

This paper presents a DDPG reinforcement learning framework for online adaptive tuning of sliding mode control gains in a nonlinear magnetic levitation system. The SMC provides inherent robustness to uncertainties and disturbances, while the DDPG agent continuously adjusts the sliding surface coefficients, switching gain, and boundary

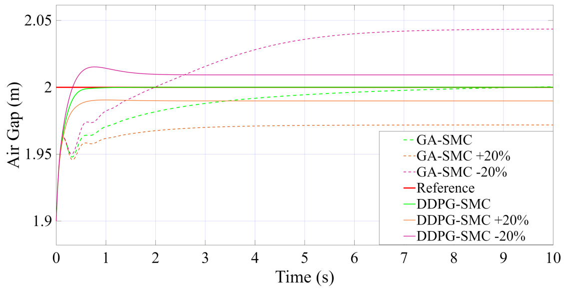

Fig. 9: Air gap x_1 under $\pm 20\%$ mass variation: DDPG-SMC vs. GA-SMC.

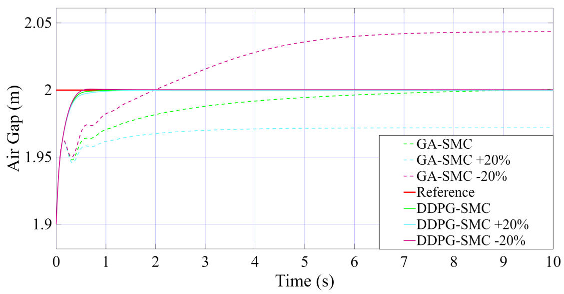

Fig. 10: Air gap x_1 under $\pm 20\%$ resistance variation: DDPG-SMC vs. GA-SMC.

layer in real time based on system state feedback. Lyapunov stability is established for the fixed-gain case; the time-varying gain scenario arising from online adaptation is identified as a limitation and a direction for future theoretical investigation.

Simulation results demonstrate that DDPG-SMC achieves superior tracking performance, faster settling time, and smoother control effort compared to GA-SMC. Disturbance rejection tests show that DDPG-SMC limits velocity deviations to within ± 0.2 kg·m/s against disturbances that cause ± 0.7 kg·m/s oscillations in GA-SMC. Parameter uncertainty tests under $\pm 20\%$ variations in mass and resistance confirm that DDPG-SMC maintains near-reference tracking while GA-SMC exhibits persistent steady-state error.

Despite these promising results, several limitations remain. The framework is validated entirely in MATLAB/Simulink and has not been tested on physical hardware, where sensor noise, actuator delays, and real-time computational constraints may affect performance. The Lyapunov stability proof applies only to the fixed-gain case, and a formal guarantee for the time-varying adaptive scenario is currently unavailable. Future work will address formal stability analysis under adaptive gains, hardware validation on real-time platforms, extension to other underactuated nonlinear systems, and comparative evaluation against recent adaptive SMC methods from the literature to further benchmark the contribution of the proposed framework.

ACKNOWLEDGMENT

The authors thank the National University of Sciences and Technology, Islamabad, for supporting this research.

REFERENCES

[1] J. Xu, Y. Sun, D. Gao, W. Ma, S. Luo, and Q. Qian, "Dynamic modeling and adaptive sliding mode control for a maglev train system based on a magnetic flux observer," *IEEE Access*, vol. 6, pp. 31 571–31 579, 2018.

[2] A. Mahmood, H. Dulaimi, H. Al-Khazraji, N. Farhan, M. Mustafa, M. Ahmed, and H. Saleh, "Nonlinear tracking motion control based multi-verse optimization for magnetic levitation systems," *International Journal of Mechatronics and Applied Mechanics*, vol. 2026, pp. 285–293, 2026.

[3] A. M. Dongardive, H. R. Mane, R. H. Chile, and S. T. Hamde, "Design of super-twisting disturbance observer-based controller for magnetic levitation system," *International Journal of Dynamics and Control*, vol. 11, no. 3, pp. 1190–1202, 2023.

[4] W. Yang, F. Meng, S. Meng, S. Man, and A. Pang, "Tracking control of magnetic levitation system using model-free rbf neural network design," *IEEE Access*, vol. 8, pp. 204 563–204 572, 2020.

[5] A. Ma'arif, M. A. M. Vera, M. S. Mahmoud, E. Umoh, A. J. Abougarair, and S. N. Rahmadhia, "Sliding mode control design for magnetic levitation system," *Journal of Robotics and Control*, vol. 3, no. 6, pp. 848–853, 2023.

[6] H. M. S. Yaseen, S. A. Siffat, I. Ahmad, and A. S. Malik, "Nonlinear adaptive control of magnetic levitation system using terminal sliding mode and integral backstepping sliding mode controllers," *ISA Transactions*, vol. 126, pp. 121–133, 2022.

[7] A. K. Hamoudi and L. T. Rasheed, "Backstepping sliding mode control for magnetic levitation position control: Design and analysis," *Mathematical Modelling of Engineering Problems*, vol. 12, no. 3, pp. 2488–2500, 2025.

[8] H. M. M. Adil, S. Ahmed, and I. Ahmad, "Control of maglev system using supertwisting and integral backstepping sliding mode algorithm," *IEEE Access*, vol. 8, pp. 80 235–80 246, 2020.

[9] Y. Wang, D. Zhou, J. Li, M. Song, and Q. Yang, "Integral backstepping and lyapunov calm control design for magnetic levitation system," in *Proceedings of the 40th Chinese Control Conference (CCC)*, Shanghai, China, 2021, pp. 674–678.

[10] H. M. M. Adil, "Control of maglev system using double integral barrier-based adaptive sliding mode algorithm," in *Proceedings of the 1st International Conference on Innovative Engineering Sciences and Technological Research (ICIESTR)*, 2024, pp. 1–6.

[11] D. K. Singh, S. Jamuar, S. Ansari, and S. Manna, "Robust adaptive optimal feedback based integral sliding mode controller for magnetic levitation system," in *Proceedings of the IEEE ICE2CPT Conference*, 2025, pp. 1–5.

[12] M. Jastrzebski and J. Kabziński, "Adaptive control of magnetic levitation system based on fuzzy inversion," *Scientific Reports*, vol. 14, no. 1, p. 24815, 2024.

[13] D. E. Goldberg, *Genetic Algorithms in Search, Optimization, and Machine Learning*. Reading, MA: Addison-Wesley, 1989.

[14] M. A. Faraj, M. J. Mahammad, and S. Jassam, "Backstepping sliding mode controller design for magnetic levitation system based on fractional order theory and zebra optimization algorithm," *Journal of Robotics and Control*, vol. 6, no. 5, pp. 2488–2500, 2025.

[15] A. Mughees and S. A. Mohsin, "Design and control of magnetic levitation system by optimizing fractional order pid controller using ant colony optimization algorithm," *IEEE Access*, vol. 8, pp. 113 410–113 422, 2020.

[16] L. Zheng, Y. Wang, R. Yang, S. Wu, R. Guo, and E. Dong, "An efficiently convergent deep reinforcement learning-based trajectory planning method for manipulators in dynamic environments," *Journal of Intelligent & Robotic Systems*, vol. 107, no. 4, p. 50, 2023.

[17] T. P. Lillicrap, J. J. Hunt, A. Pritzel, N. Heess, T. Erez, Y. Tassa, D. Silver, and D. Wierstra, "Continuous control with deep reinforcement learning," in *Proc. 4th International Conference on Learning Representations (ICLR)*, San Juan, Puerto Rico, 2016, arXiv:1509.02971.

[18] M. Zhang, H. Zang, and Z. Liu, "Fractional-order adaptive sliding mode control based on predefined-time stability for chaos synchronization," *Chaos, Solitons & Fractals*, vol. 191, p. 115921, 2025.